Total Energy in Supernova Neutrinos and the Tidal Deformability and Binding Energy of Neutron Stars

Brendan Reed[1, 2, *] and C. J. Horowitz[2, †]

[1]*Department of Astronomy, Indiana University, Bloomington, IN 47405, USA*
[2]*Center for Exploration of Energy and Matter and Department of Physics,*
Indiana University, Bloomington, IN 47405, USA

(Dated: October 13, 2020)

The energy radiated in supernova neutrinos is a fundamental quantity that is closely related to the gravitational binding energy of a neutron star. Recently the tidal deformability of neutron stars was constrained by gravitational wave observations. By considering several equations of state, we find a strong correlation between the tidal deformability and neutron star binding energy. We use this correlation to sharpen predictions of the binding energy of neutron stars and the total neutrino energy in supernovae. We find a minimum binding energy for a neutron star formed in a supernova of $\sim 1.5 \times 10^{53}$ ergs. Should the neutrino energy in a supernova be significantly below this value, it would strongly suggest new unobserved particles are carrying away some of the supernova energy. Alternatively, if the neutrino energy is observed above $\sim 6 \times 10^{53}$ ergs, it would strongly imply the formation of a (perhaps surprisingly) massive neutron star.

I. INTRODUCTION

The next galactic core collapse supernova (SN) will be a watershed event. This SN may be an important gravitational wave source that could be the first multi-messenger event with gravitational wave, neutrino, and electromagnetic detections. The observation of about 20 neutrinos during SN1987A constrained the total neutrino energy to be $2 - 4 \times 10^{53}$ ergs [1, 2]. However, this event had both large statistical and systematic errors and only electron antineutrinos were likely observed. Other neutrino flavors carried away significant energy and their unmeasured spectra and luminosities contribute substantially to systematic errors.

Modern neutrino detectors should observe many thousands of events from a SN at 10 kpc, dramatically increasing the statistics compared to SN1987A. Large neutrino detectors such as Super-Kamiokande [3] and Hyper-Kamiokande [4] should provide excellent statistics on $\bar{\nu}_e$ while DUNE [5] will be a good ν_e detector. To determine the total neutrino energy it is important to also measure muon and tauon neutrinos and antineutrinos. This can be done via neutrino-nucleus elastic scattering [6]. Although the nuclear recoils in these detectors have low energies, the coherent cross section is very large, one is sensitive to all flavors of (active) neutrinos, and the bulk of the detector mass contributes. As a result elastic scattering detectors can have yields of tens of events per *ton* for a SN at 10 kpc compared to 100s of events per *kilo-ton* for a conventional detector [6].

A number of large dark matter detectors are now sensitive to a galactic SN via neutrino-nucleus elastic scattering. Furthermore larger detectors, that are

presently under construction or planned, should improve the statistics. Detectors using Xe include Xenon1T [7, 8], XenonnT, and DARWIN [9]. Large Ar detectors include Deap-3600 [10], Dark-Side, DarkSide-20k [11] and ARGO [12]. A tens of tons dark matter detector with low threshold and good control of systematic errors can be a powerful supernova observatory and may be able to determine the total energy in active neutrinos to better than 10 percent [13]. In addition, RES-NOVA is a very promising idea for a Lead-based coherent scattering detector [14].

In this work, we focus on the total energy in (active) neutrinos radiated by a galactic SN. This is a fundamental quantity that is insensitive to (active) neutrino oscillations and will be important for many analyses. The total neutrino energy is closely related to the gravitational binding energy, E_b, of the newly formed neutron star (NS). If the total energy is observed to be low this could strongly suggest that new unobserved particles, such as sterile neutrinos or axions, carry away the remainder of the binding energy [15, 16]. Alternatively, if the energy is large it may uniquely signal the formation of a (perhaps unexpectedly) massive neutron star.

The binding energy of a neutron star has uncertainties from uncertainties in the equation of state (EOS). The EOS of dense matter governs the structure and behavior of nuclear matter in both macroscopic (e.g. neutron stars) and microscopic (e.g. atomic nuclei) systems. While the exact form of the EOS of dense matter is not fully understood, a great number of effective formalisms have been used to accurately predict the behavior of many macroscopic and microscopic nuclear systems. The EOS of nuclear matter has only been fully probed in laboratory experiments near saturation density, $\rho_0 \approx 0.15$ fm^{-3}, and so one must look to astrophysical systems such as neutron stars to further probe the EOS. In the high density regime of a neutron star, the nuclear matter behaves at the zero temperature ("cold") limit and can

*Electronic address: reedbr@iu.edu
†Electronic address: horowit@indiana.edu

reach densities that are several times saturation density.

Many astronomical radio [17, 18], X-ray [19] and gravitational wave [20, 21] observations have been able to provide constraints on neutron star observables and the high density EOS. Some NS observables closely related to the EOS are the mass (M), radius (R), moment of inertia (I), and dimensionless tidal polarizability (Λ). The *tidal polarizability* (or deformability) is an intrinsic NS property highly sensitive to the stellar compactness $\xi = 2GM/R$ [22–27] that describes the tendency of a NS to develop a mass quadrupole as a response to the tidal field induced by its companion [28, 29]. The dimensionless tidal polarizability Λ is defined as follows,

$$\Lambda = \frac{2}{3}k_2\Big(\frac{R}{GM}\Big)^5 = \frac{64}{3}k_2\Big(\frac{R}{R_s}\Big)^5 \qquad (1)$$

where k_2 is the second Love number [30, 31], and M and R are the neutron star mass and radius, respectively, and $R_s = 2GM$. The limit on the deformability of a $1.4\mathrm{M}_\odot$ NS at 90% confidence from GW170817 is $\Lambda_{1.4} = 190^{+390}_{-120}$ [32]. This tidal deformability measurement rules out several previously viable EOSs [20]. Below, we show that this also improves our knowledge of the binding energy of neutron stars and increases the utility of measuring the total neutrino energy in a SN.

In this paper, we explore connections between E_b and the tidal deformability Λ. Since both quantities are linked to the stellar compactness, we believe that constraints on either quantity from future observations can have meaningful constraints on the other. Note that Sun *et al.* have explored the relationship between E_b and compactness [33]. In Sec. II, we detail the calculation of the gravitational binding energy of a NS and the dimensionless tidal deformability for various EOSs. Our selection of EOSs include both relativistic and non-relativistic models. We present our results including the behavior of E_b on the deformability of a $1.4\,M_\odot$ NS ($\Lambda_{1.4}$) and on the mass of the NS in Sec. III. We discuss our results and implications for future supernova neutrino observations in Sec. IV and conclude in Sec. V. We use standard units where $c = \hbar = 1$.

II. FORMALISM

We calculate the binding energy of a NS in Sec. II A and deformability in Sec. II B. See Table I for a complete list of all EOSs used in this work. We chose this particular set of EOS as they predict a broad range of different properties of finite nuclei and NSs, in particular the maximum masses and the radii of $1.4\,M_\odot$ NSs explore a wide range of values, see Fig. 1. This is by no means an exhaustive list of all possible NS EOS, however it does provide a range of very different predictions for both NS and finite nuclei properties.

For building our relativistic NS EOS, we adopt the Duflo-Zuker mass table for the outer crust defined up to a density of 4.3×10^{11} g cm^{-3} [50]. The inner crust is

EOS	$\Lambda_{1.4}$	$E_b(1.174\,M_\odot)$ [10^{53} erg]	$E_b(1.4\,M_\odot)$ [10^{53} erg]	$E_b(2\,M_\odot)$ [10^{53} erg]
APR [34]	252.7	1.82	2.74	6.51
BSk20 [35]	323.7	1.78	2.65	6.24
BSk21 [35]	516.1	1.68	2.48	5.65
Big Apple [36]	713.0	1.62	2.38	5.26
FPS [37]	177.4	1.86	2.82	–
FSUGold 2 [38]	874.1	1.44	2.14	4.97
FSUGold 2H [39]	782.6	1.60	2.35	5.21
FSUGold 2R [39]	617.0	1.62	2.38	5.46
FSUGarnet [40]	642.7	1.61	2.38	5.43
GNH3 [41]	1094.6	1.31	1.98	–
IUFSU [42]	507.6	1.65	2.44	–
IUFSU2 [43]	562.7	1.64	2.42	5.55
MPA1 [44]	563.3	1.75	2.57	5.77
NL3 [45]	1266.6	1.42	2.08	4.60
NL3$\omega\rho$ (.209) [46]	952.2	1.54	2.25	4.94
SLy [47]	320.1	1.72	2.59	6.28
TAMUa [48]	730.8	1.50	2.23	5.15
TAMUb [48]	979.6	1.40	2.07	4.79
WFF2 [49]	229.0	1.92	2.86	6.76

TABLE I: Table of fiducial values for the EOSs used in the text. Missing values are when the EOS does not support a $2\mathrm{M}_\odot$ NS.

calculated by interpolating between the outer crust and liquid core with a cubic polynomial which is continuous in both the pressure and in the speed of sound [51]. The core-crust transition density is given from the RPA formalism described in [46]. Note that a number of these EOSs were downloaded from the web page of Feryal Özel [52].

A. Neutron Star Binding Energy

We define the gravitational mass of a NS to be the mass observed at infinity. This quantity is calculated by solving

$$M = \int_0^R 4\pi r^2 \rho(r)dr \qquad (2)$$

in conjunction with the Tolman-Oppenheimer-Volkoff (TOV) equations to solve for the structure of a NS [53, 54]. Here, $\rho(r)$ is the energy density of matter.

For a non-rotating NS, the volume element in the Schwarzschild metric takes the form

$$dV = 4\pi r^2 \Big[1 - \frac{2GM(r)}{r}\Big]^{-1/2} dr \qquad (3)$$

thereby making the total number of baryons calculated from

$$A = \int_0^R 4\pi r^2 n(r) \Big[1 - \frac{2GM(r)}{r}\Big]^{-1/2} dr \qquad (4)$$

where $n(r)$ is the number density of baryons at a radius r. The baryonic mass of a NS can then be defined as the

total mass of A baryons, generally $M_b = m_\star A$ where $m_\star$ is the mass of a baryon (939 MeV) [55–57].

The binding energy of a NS is defined as the total amount of energy required to assemble A baryons from infinity to form a stable star. This quantity can be measured via supernova neutrinos, which radiate approximately 99% of the gravitational energy released from a core-collapse at the end of a massive star's life [56, 58]. Since the collapsing object starts as a white-dwarf-like iron core, the total effective binding energy is calculated starting not from an ensemble of free baryons, but instead from iron nuclei,

$$E_b = M - A\tilde{m}, \tag{5}$$

where $\tilde{m}$ is the effective mass per baryon, taken to be the mass of $^{56}\mathrm{Fe}/56 = 930.412$ MeV [56]. We adopt a positive value for the binding energy and hereafter, references to "binding energy" will refer to the effective binding energy given by Eq. 5.

B. Tidal Deformability Calculation

We now detail the deformability calculation. After one solves the TOV equations for the structure of a NS, we then calculate the second tidal Love number k_2 to solve for Λ. The second tidal Love number is calculated via

$$
\begin{aligned}
k_2 = \frac{1}{20}\xi^5(1-\xi)^2 &\Big[(2-y_R)+(y_R-1)\xi\Big] \times \\
&\left\{\left[(6-3y_R)+\frac{3}{2}(5y_R-8)\xi\right]\xi + \right. \\
\frac{1}{2}\Big[(13-11y_R)+\frac{1}{2}(3y_R-2)\xi&+\frac{1}{2}(1+y_R)\xi^2\Big]\xi^2+ \\
3\Big[(2-y_R)+(y_R-1)\xi\Big]&(1-\xi)^2\ln(1-\xi)\bigg\}^{-1}.
\end{aligned} \tag{6}
$$

Here ξ is the stellar compactness defined as before as $\xi = 2GM/R$ and $y_R = y(R)$ is a dimensionless quantity which is calculated by solving the nonlinear differential equation,

$$r\frac{dy}{dr} + y^2 + F(r)y + r^2 Q(r) = 0 \tag{7}$$

with the initial condition $y(0) = 2$. The functions $F(r)$ and $Q(r)$ are given below [22, 51],

$$F(r) = \frac{r - 4\pi Gr^3(\rho(r)-p(r))}{r - 2GM(r)}, \tag{8}$$

$$
\begin{aligned}
Q(r) = \frac{4\pi r}{r-2GM(r)}&\left[G\Big(5\rho(r)+9p(r)+\frac{\rho(r)+p(r)}{c_s^2(r)}\Big)\right. \\
&\left.-\frac{6}{4\pi r^2}\right] - 4\left[\frac{G(M(r)+4\pi r^3 p(r))}{r(r-2GM(r))}\right]^2.
\end{aligned} \tag{9}
$$

For a given EOS, we calculate the binding energy from Eqs. 2, 4, and 5 and the deformability from Eqs. 1 and 6 with y_R from the solution to Eq. 7.

III. RESULTS

We first show in Fig. 2 the calculated binding energies for four of the twenty EOSs used in this study. We choose to plot E_b against ξ to illustrate its correlation with the stellar compactness. These EOSs were chosen so that we probe a variety of both relativistic (e.g. FSUGold 2 [38] and NL3 [45]) and non-relativistic (e.g. SLy [47] and APR [34]) formalisms. All EOSs along with fiducial values for the deformability and binding energies can be found in Table I.

We then plot the behavior of E_b and $\Lambda_{1.4}$ for fixed values of M in Figs. 3-5. These figures reveal a linear correlation between E_b and $\Lambda_{1.4}$ for a fixed value of M. If one were to fix $\Lambda_{1.4}$, this may provide a simple way to estimate the binding energy or gravitational mass should one observe either quantity more stringently. A simple least-squares fit $E_b \approx a_1\Lambda_{1.4} + a_2$ yields the parameters a_1 and a_2 along with the 1σ and 2σ error bands as shown in Figs. 3-5. The 1σ values are calculated from the estimated covariance matrix generated using the SciPy [59] package curve_fit() [60], which uses the Levenberg-Marquardt minimization routine to obtain an optimal parameter set. The 2σ values are then just twice the 1σ values.

These error regions can then be used to display the dependency of E_b on M and provide a way to estimate either if one fixes $\Lambda_{1.4}$. As our knowledge of $\Lambda_{1.4}$ improves, a measurement of E_b more sharply constrains M. To illustrate this, we use the linear fits described above to calculate a 1σ band of values for E_b at different values of M for a few characteristic values of $\Lambda_{1.4}$ in Fig. 6. We observe a strongly constrained band of E_b values at each M for each of the characteristic $\Lambda_{1.4}$ values. For example, should future gravitational wave observations constrain $\Lambda_{1.4}$ to be very close to the GW170817 central value ≈ 190, this band becomes further constrained to higher values of E_b with less uncertainty. For comparison, we also show the estimates of E_b and the remnant mass from SN1987a [1, 2].

We conclude these results by presenting constraints on the binding energy of low mass NSs. We show the calculated E_b values for a few different mass NSs, fixing $\Lambda_{1.4} = 580$ in Table II and $\Lambda_{1.4} = 190$ in Table III. In particular, we show the E_b for the lowest observed NS mass of $1.174 \pm 0.004\,M_\odot$ [61]. We find that based on our linear fitting procedure above, the lowest mass neutron star must have a binding energy $\gtrsim 1.5 \times 10^{53}$ erg.

IV. DISCUSSION AND IMPLICATIONS

We will now discuss the implications of our findings. Firstly, the gravitational binding energy is correlated with the deformability $\Lambda_{1.4}$. This correlation can be used to calculate an expected range of values for E_b at a given M. Different values for $\Lambda_{1.4}$ predict different curves for the behavior of E_b and this can be used to place con-
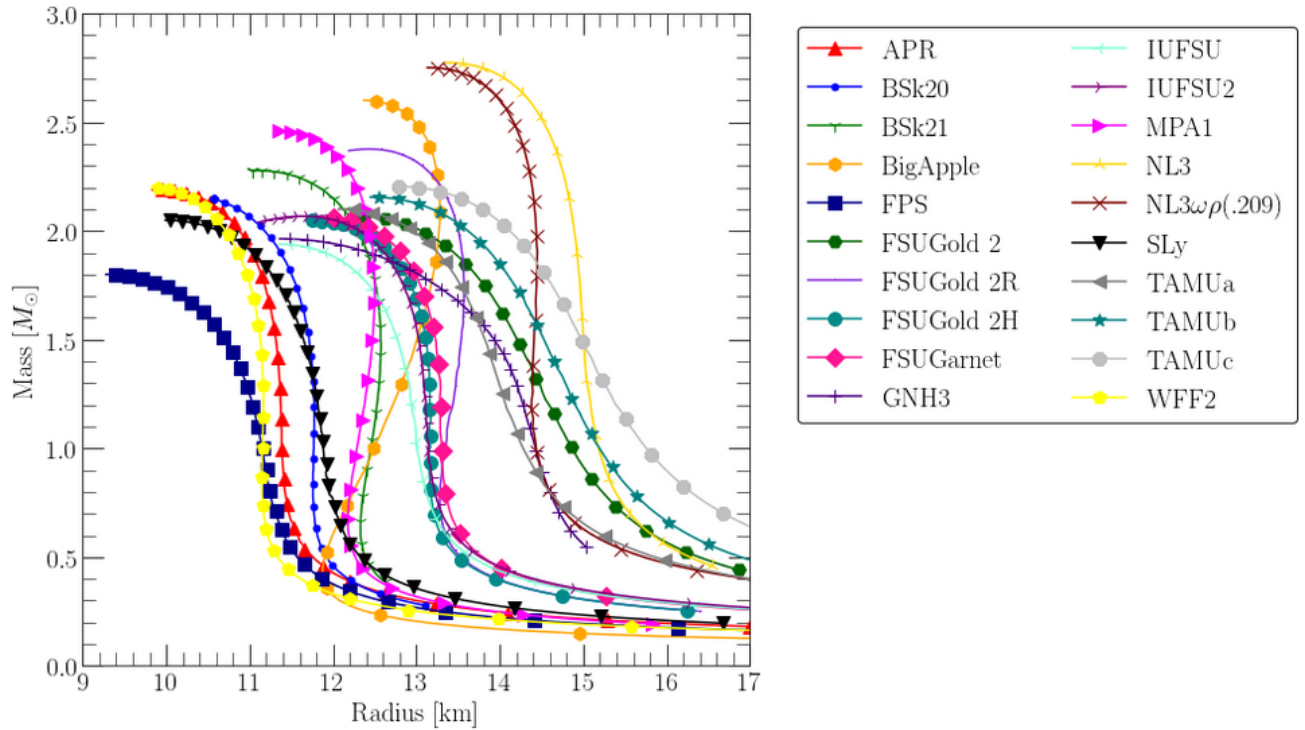
FIG. 1: Mass-radius plot for the full set of EOS used in this study. The key for each EOS color and marker shape shall be used throughout the remainder of the figures in this paper.

Mass	$E_b(\Lambda_{1.4} = 580)$	2σ Range
$[M_\odot]$	$[10^{53}$ erg$]$	$[10^{53}$ erg$]$
1.0	1.16 ± 0.044	$[1.067, 1.244]$
1.174	1.65 ± 0.057	$[1.539, 1.766]$
1.4	2.45 ± 0.076	$[2.302, 2.606]$
1.8	4.41 ± 0.144	$[4.120, 4.697]$
2.0	5.68 ± 0.191	$[5.294, 6.057]$

TABLE II: Estimated binding energies for different remnant masses assuming a deformability of $\Lambda_{1.4} = 580$. The middle column shows the 1σ error while the right column shows the 2σ range of binding energies for the given remnant mass.

Mass	$E_b(\Lambda_{1.4} = 190)$	2σ Range
$[M_\odot]$	$[10^{53}$ erg$]$	$[10^{53}$ erg$]$
1.0	1.29 ± 0.031	$[1.228, 1.352]$
1.174	1.85 ± 0.040	$[1.771, 1.930]$
1.4	2.76 ± 0.053	$[2.656, 2.869]$
1.8	5.03 ± 0.101	$[4.823, 5.228]$
2.0	6.49 ± 0.134	$[6.223, 6.760]$

TABLE III: Same as Table II but for $\Lambda_{1.4} = 190$.

straints on either $\Lambda_{1.4}$ or E_b should the other become better constrained. As our knowledge of $\Lambda_{1.4}$ grows from additional gravitational wave observations, E_b will become better constrained. This increases the utility of measuring the total energy in active neutrinos during the next galactic supernova.

Since the range of E_b predicted is fairly well con-

strained at each M, this allows important tests for new physics. For instance, the existence of new exotic particles beyond the standard model may affect the energetics of the supernova. The lowest, well measured, neutron star mass is $1.174 \pm 0.004 M_\odot$ [61]. The existence of such a low mass NS has provided a challenge for supernova simulations as it is difficult to achieve such a low-mass remnant [62]. It may also be difficult to produce a much lighter NS in a SN because the star's core must reach the Chandrasekhar mass, $\approx 1.4\,M_\odot$, in order to collapse, and the SN shock may only remove a small fraction of this mass. This leaves behind a NS not significantly lighter than $1.174 M_\odot$.

We find an important *lower bound* on E_b for a NS. Constraints on $\Lambda_{1.4} < 580$ now rule out stiff equations of state that predict low E_b. For $\Lambda_{1.4} = 580$, we find a 2σ lower bound for a $1.174 M_\odot$ star of $E_b > 1.52 \times 10^{53}$ ergs. This provides a *lower bound on the energy radiated in active neutrinos* during a SN. If the observed energy is significantly less than this bound, it is very likely some of the NS binding energy went into new unobserved particles such as sterile neutrinos, axions, or other light dark matter constituents [15, 16]. This emphasizes that the total energy in neutrinos during a SN is a fundamental quantity that is very important to measure well.

The gravitational wave event GW190814 involved a $2.6 M_\odot$ compact object that could be the most massive neutron star observed [63], although subsequent analyses disfavor this hypothesis [36, 64–67]. Nevertheless, a
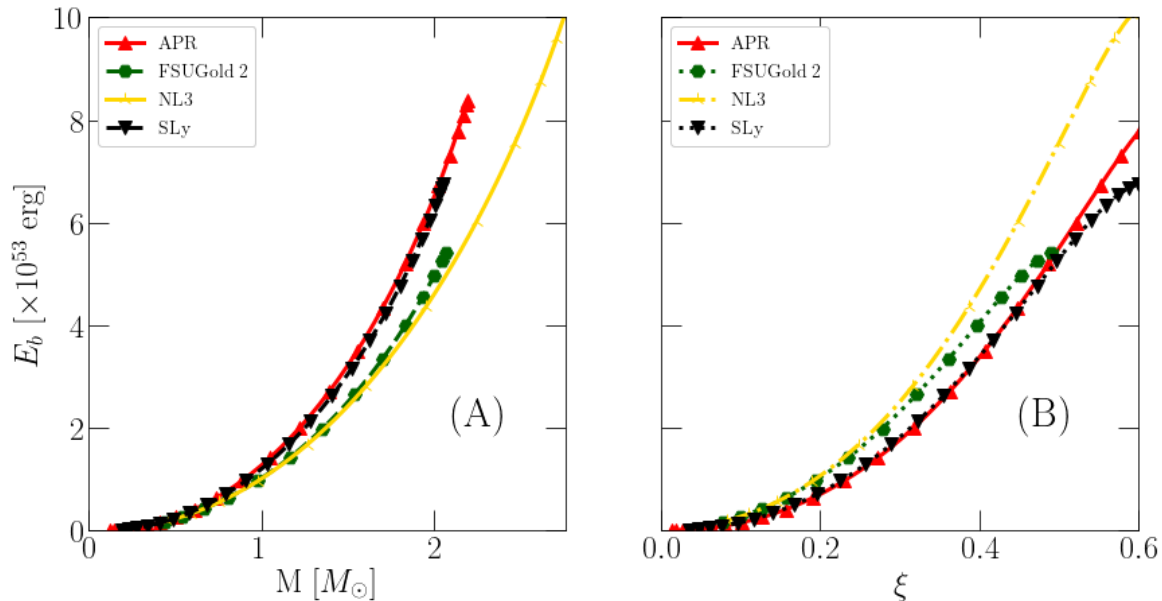
FIG. 2: Gravitational binding energy versus stellar mass (A) and compactness $\xi = 2GM/R$ (B) for four EOSs considered in the text. Fiducial values for all EOS can be found in Table I.

supernova birthing such a massive NS would radiate an extremely large energy in neutrinos. We can see from Fig. 2 that most EOS predict a NS maximum mass of $\sim$2 $M_\odot$ with a binding energy of $\sim$5-7 $\times 10^{53}$ erg. However, two EOS used here predict a maximum mass $\geq 2.6\,M_\odot$ with E_b in excess of 10^{54} erg. If the energy in neutrinos from a supernova significantly exceeds $\sim 6 \times 10^{53}$ erg, this would almost uniquely imply the formation of a very massive NS.

V. CONCLUSION

We have used several different equations of state to predict that the binding energy of a neutron star E_b is correlated with the tidal deformability. Using our correlation and the LIGO gravitational wave constraint on the deformability of a $1.4M_\odot$ NS of $\Lambda_{1.4} = 190^{+390}_{-120}$, we determine a range of binding energies expected for a given neutron star mass. This range will be further constrained as $\Lambda_{1.4}$ becomes better determined with future gravita-

tional wave observations. The total energy radiated in neutrinos during a SN is closely related to E_b. This reduction in the uncertainty in E_b increases the utility and importance of accurately measuring the total energy in neutrinos from the next SN. If the total energy is significantly less than $\sim 1.5 \times 10^{53}$ ergs it may strongly suggest that new particles are carrying away some of the SN energy. Alternatively if the energy is unexpectedly large, it may uniquely imply the formation of a surprisingly massive NS.

Acknowledgments

[1] K. Hirata, T. Kajita, M. Koshiba, M. Nakahata, Y. Oyama, N. Sato, A. Suzuki, M. Takita, Y. Totsuka, T. Kifune, et al., Phys. Rev. Lett. **58**, 1490 (1987).
[2] R. M. Bionta, G. Blewitt, C. B. Bratton, D. Casper, A. Ciocio, R. Claus, B. Cortez, M. Crouch, S. T. Dye, S. Errede, et al., Phys. Rev. Lett. **58**, 1494 (1987).
[3] Y. Fukuda et al. (Super-Kamiokande), Nucl. Instrum.

Meth. A **501**, 418 (2003).
[4] K. Abe et al. (Hyper-Kamiokande) (2018), 1805.04163.
[5] M. Goodman, Adv. High Energy Phys. **2015**, 256351 (2015).
[6] C. J. Horowitz, K. J. Coakley, and D. N. McKinsey, Phys. Rev. D **68**, 023005 (2003), URL https://link.aps.org/doi/10.1103/PhysRevD.68.023005.
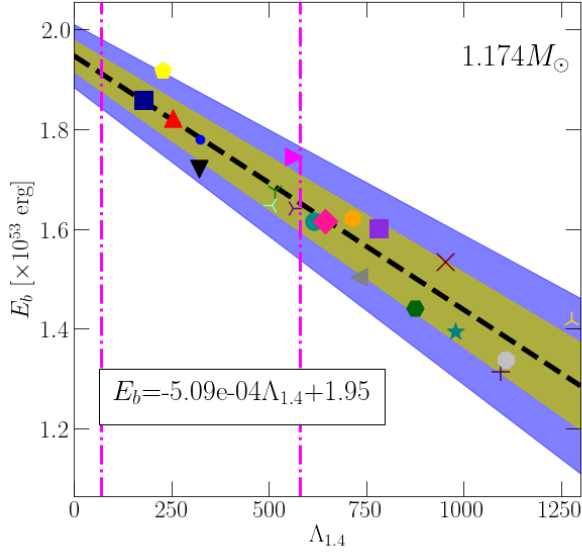
FIG. 3: Binding energy of a $1.174\,M_\odot$ NS versus $\Lambda_{1.4}$. The vertical dot-dashed lines show the upper and lower limits on $\Lambda_{1.4}$ from analysis of GW170817 [20]. The dashed line is the linear least-squares best fit with the yellow and blue regions marking the 1σ and 2σ errors on the fit respectively. The equation results from a linear least-squares fit, with E_b in units of 10^{53} erg.
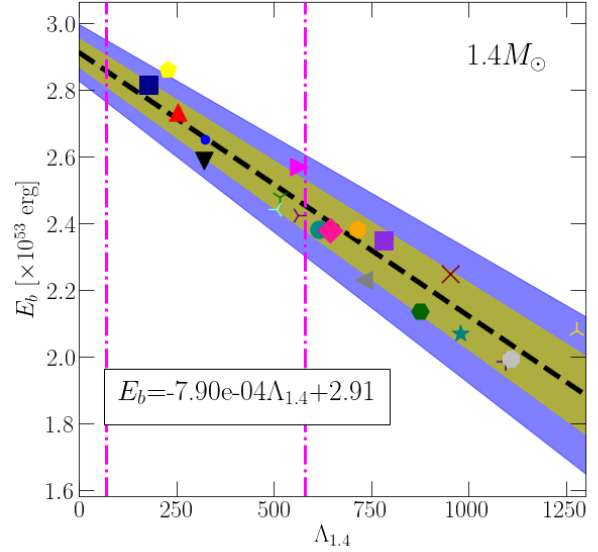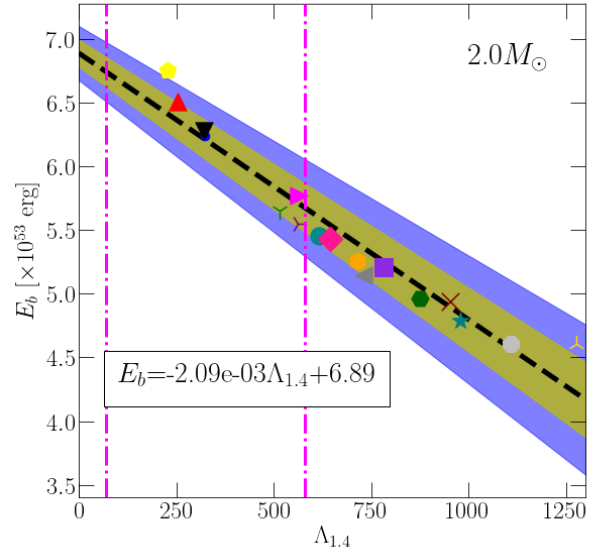

FIG. 4: Same as Fig. 3 but for $1.4\,M_\odot$ star.

FIG. 5: Same as Fig. 3 but for $2.0\,M_\odot$ star.

[7] E. Aprile, J. Aalbers, F. Agostini, M. Alfonsi, F. D. Amaro, M. Anthony, L. Arazi, F. Arneodo, C. Balan, P. Barrow, et al., Journal of Cosmology and Astroparticle Physics **2016**, 027 (2016).

[8] E. Aprile et al. (XENON) (2020), 2006.09721.

[9] J. Aalbers, F. Agostini, M. Alfonsi, F. Amaro, C. Amsler, E. Aprile, L. Arazi, F. Arneodo, P. Barrow, L. Baudis, et al., Journal of Cosmology and Astroparticle Physics **2016**, 017 (2016).

[10] R. Ajaj, P.-A. Amaudruz, G. R. Araujo, M. Baldwin, M. Batygov, B. Beltran, C. E. Bina, J. Bonatt, M. G. Boulay, B. Broerman, et al. (DEAP Collaboration), Phys. Rev. D **100**, 022004 (2019), URL https://link.aps.org/doi/10.1103/PhysRevD.100.022004.

[11] C. E. Aalseth, F. Acerbi, P. Agnes, I. F. M. Albuquerque, T. Alexander, A. Alici, A. K. Alton, P. Antonioli, S. Arcelli, R. Ardito, et al., The European Physical Journal Plus **133**, 131 (2018), URL https://doi.org/10.1140/epjp/i2018-11973-4.

[12] M. C. Gonzalez-Garcia, M. Maltoni, Y. F. Perez-Gonzalez, and R. Z. Funchal, Journal of High Energy Physics **2018**, 19 (2018), URL https://doi.org/10.1007/JHEP07(2018)019.

[13] R. F. Lang, C. McCabe, S. Reichard, M. Selvi, and I. Tamborra, Phys. Rev. D **94**, 103009 (2016), URL https://link.aps.org/doi/10.1103/PhysRevD.94.103009.

[14] L. Pattavina, N. F. Iachellini, and I. Tamborra (2020), 2004.06936.

[15] J. H. Chang, R. Essig, and S. D. McDermott, Journal of High Energy Physics **2018**, 51 (2018), URL https://doi.org/10.1007/JHEP09(2018)051.

[16] G. Raffelt and D. Seckel, Phys. Rev. Lett. **60**, 1793 (1988), URL https://link.aps.org/doi/10.1103/PhysRevLett.60.1793.

[17] P. B. Demorest, T. Pennucci, S. M. Ransom, M. S. E. Roberts, and J. W. T. Hessels, Nature **467**, 1081 EP (2010), URL https://doi.org/10.1038/nature09466.

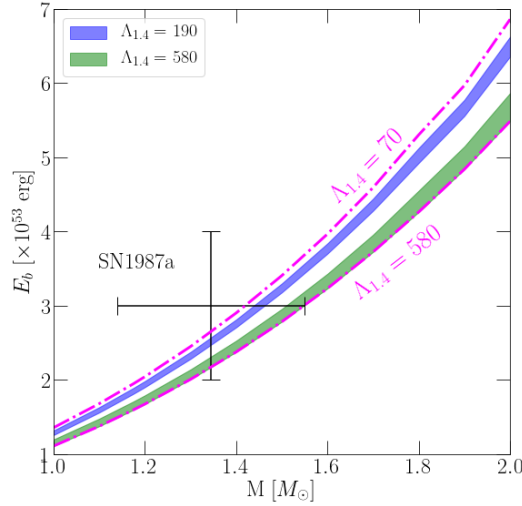[18] H. T. Cromartie, E. Fonseca, S. M. Ransom, P. B.

FIG. 6: Binding energy as a function of remnant mass at various fixed deformabilities. The blue and green bands show the 1σ confidence intervals based on the linear fits described in Sec. III for $\Lambda_{1.4} = 190$ and 580 respectively. The black error bars represent the constraints from SN1987a [1, 2]. The dash-dot pink curves represent the bounds of allowed E_b for deformabilities in the range $\Lambda_{1.4} = [70, 580]$.

Demorest, Z. Arzoumanian, H. Blumer, P. R. Brook, M. E. DeCesar, T. Dolch, J. A. Ellis, et al., Nature Astronomy (2019), URL https://doi.org/10.1038/s41550-019-0880-2.

[19] M. C. Miller, F. K. Lamb, A. J. Dittmann, S. Bogdanov, Z. Arzoumanian, K. C. Gendreau, S. Guillot, A. K. Harding, W. C. G. Ho, J. M. Lattimer, et al., The Astrophysical Journal 887, L24 (2019), URL https://doi.org/10.3847%2F2041-8213%2Fab50c5.

[20] B. P. Abbott et al. (Virgo, LIGO Scientific), Phys. Rev. Lett. 119, 161101 (2017).

[21] B. P. Abbott, R. Abbott, T. D. Abbott, S. Abraham, F. Acernese, K. Ackley, C. Adams, R. X. Adhikari, V. B. Adya, C. Affeldt, et al., Astrophys. Journal Lett. 892, L3 (2020), 2001.01761.

[22] T. Hinderer, Astrophys. J. 677, 1216 (2008).

[23] T. Hinderer, B. D. Lackey, R. N. Lang, and J. S. Read, Phys. Rev. D81, 123016 (2010).

[24] T. Damour and A. Nagar, Phys. Rev. D80, 084035 (2009).

[25] S. Postnikov, M. Prakash, and J. M. Lattimer, Phys. Rev. D82, 024016 (2010).

[26] F. J. Fattoyev, J. Carvajal, W. G. Newton, and B.-A. Li, Phys. Rev. C87, 015806 (2013).

[27] A. W. Steiner, S. Gandolfi, F. J. Fattoyev, and W. G. Newton, Phys. Rev. C91, 015804 (2015).

[28] T. Damour, M. Soffel, and C. Xu, Phys. Rev. D45, 1017 (1992).

[29] E. E. Flanagan and T. Hinderer, Phys. Rev. D77, 021502 (2008).

[30] T. Binnington and E. Poisson, Phys. Rev. D80, 084018 (2009).

[31] T. Damour, A. Nagar, and L. Villain, Phys. Rev. D85, 123007 (2012).

[32] B. P. Abbott, R. Abbott, T. D. Abbott, F. Acernese, K. Ackley, C. Adams, T. Adams, P. Addesso, R. X. Adhikari, V. B. Adya, et al. (The LIGO Scientific Collaboration and the Virgo Collaboration), Phys. Rev. Lett. 121, 161101 (2018), URL https://link.aps.org/doi/10.1103/PhysRevLett.121.161101.

[33] W. Sun, D. Wen, and J. Wang, Phys. Rev. D 102, 023039 (2020), URL https://link.aps.org/doi/10.1103/PhysRevD.102.023039.

[34] A. Akmal, V. R. Pandharipande, and D. G. Ravenhall, Phys. Rev. C 58, 1804 (1998), nucl-th/9804027.

[35] A. Y. Potekhin, A. F. Fantina, N. Chamel, J. M. Pearson, and S. Goriely, Astronomy & Astrophysics 560, A48 (2013), 1310.0049.

[36] F. J. Fattoyev, C. J. Horowitz, J. Piekarewicz, and B. Reed, arXiv e-prints arXiv:2007.03799 (2020), 2007.03799.

[37] B. Friedman and V. R. Pandharipande, Nucl. Phys. A361, 502 (1981).

[38] W.-C. Chen and J. Piekarewicz, Phys. Rev. C90, 044305 (2014).

[39] L. Tolos, M. Centelles, and A. Ramos, Publications of the Astronomical Society of Australia 34, e065 (2017).

[40] W.-C. Chen and J. Piekarewicz, Phys. Lett. B748, 284 (2015).

[41] N. K. Glendenning, Astrophys. J. 293, 470 (1985).

[42] F. J. Fattoyev, C. J. Horowitz, J. Piekarewicz, and G. Shen, Phys. Rev. C82, 055803 (2010).

[43] R. Nandi, P. Char, and S. Pal, Phys. Rev. C 99, 052802 (2019), 1809.07108.

[44] H. Müther, M. Prakash, and T. L. Ainsworth, Physics Letters B 199, 469 (1987).

[45] G. A. Lalazissis, J. Konig, and P. Ring, Phys. Rev. C55, 540 (1997).

[46] J. Carriere, C. J. Horowitz, and J. Piekarewicz, Astrophys. J. 593, 463 (2003).

[47] F. Douchin and P. Haensel, Phys. Lett. B485, 107 (2000), astro-ph/0006135.

[48] F. J. Fattoyev and J. Piekarewicz, Phys. Rev. Lett. 111, 162501 (2013).

[49] R. B. Wiringa, V. Fiks, and A. Fabrocini, Phys. Rev. C38, 1010 (1988).

[50] J. Duflo and A. Zuker, Phys. Rev. C52, R23 (1995).

[51] J. Piekarewicz and F. J. Fattoyev, Phys. Rev. C 99, 045802 (2019), 1812.09974.

[52] URL http://xtreme.as.arizona.edu/neutronstars/.

[53] J. R. Oppenheimer and G. M. Volkoff, Phys. Rev. 55, 374 (1939).

[54] N. K. Glendenning, Compact Stars (Springer-Verlag New York, 2000).

[55] J. M. Lattimer and M. Prakash, Phys. Rept. 442, 109 (2007).

[56] J. M. Lattimer and M. Prakash, Astrophys. J. 550, 426 (2001), astro-ph/0002232.

[57] S. Weinberg, Gravitation and Cosmology (John Wiley & Sons, New York, 1972).

[58] M. Prakash, I. Bombaci, M. Prakash, P. J. Ellis, J. M. Lattimer, and R. Knorren, Phys. Reports 280, 1 (1997), nucl-th/9603042.

[59] P. Virtanen, R. Gommers, T. E. Oliphant, M. Haberland, T. Reddy, D. Cournapeau, E. Burovski, P. Peterson, W. Weckesser, J. Bright, et al., Nature Methods 17,

261 (2020).

[60] URL https://docs.scipy.org/doc/scipy/reference/generated/scipy.optimize.curve_fit.html.

[61] J. G. Martinez, K. Stovall, P. C. C. Freire, J. S. Deneva, F. A. Jenet, M. A. McLaughlin, M. Bagchi, S. D. Bates, and A. Ridolfi, The Astrophysical Journal **812**, 143 (2015), ISSN 1538-4357, URL http://dx.doi.org/10.1088/0004-637x/812/2/143.

[62] Y. Suwa, T. Yoshida, M. Shibata, H. Umeda, and K. Takahashi, Monthly Notices of the Royal Astronomical Society **481**, 3305 (2018), 1808.02328.

[63] R. Abbott, T. D. Abbott, S. Abraham, F. Acernese, K. Ackley, C. Adams, R. X. Adhikari, V. B. Adya, C. Af-feldt, M. Agathos, et al., The Astrophysical Journal **896**, L44 (2020), ISSN 2041-8213, URL http://dx.doi.org/10.3847/2041-8213/ab960f.

[64] I. Tews, P. T. H. Pang, T. Dietrich, M. W. Coughlin, S. Antier, M. Bulla, J. Heinzel, and L. Issa, arXiv e-prints arXiv:2007.06057 (2020), 2007.06057.

[65] Y. Lim, A. Bhattacharya, J. W. Holt, and D. Pati, arXiv e-prints arXiv:2007.06526 (2020), 2007.06526.

[66] V. Dexheimer, R. O. Gomes, T. Klähn, S. Han, and M. Salinas, arXiv e-prints arXiv:2007.08493 (2020), 2007.08493.

[67] Z. Roupas, arXiv e-prints arXiv:2007.10679 (2020), 2007.10679.